International Journal of Medical and Pharmaceutical Sciences
Open access peer-reviewed Journal
Volume 2, Issue 9, Page 1-27.
https://doi.org/10.5281/zenodo.22244992

Research Article

Design Synthesis and Development of Some Novel Pyrrole Derivatives as Antitubercular Agents

Bargaje Goraksh*, Rajeev Kumar Malviya

Faculty of Pharmacy, Mansarovar Global University, Sehore (M.P)

In the present study, we have described the design, synthesis and anti-tubercular evaluation of the series of novel pyrazole and pyrazolo[1,5-a]pyrimidine derivatives.Ligand based pharmacophore modeling study was carried out to identify critical features required for specific binding to enoyl-acyl carrier protein reductase, an important enzyme for mycobacterium cell wall synthesisThe QSAR study reveals that lipophilicity contributes major role to explain the activity. Electron withdrawing group contribute moderately while hydrogen bond donor found to contribute least. These important parameters can be taken into consideration while designing new inhibitors belonging to the above class of compounds. Generated QSAR model is statistically significant and has excellent predictive power as evidenced from the results of internal and external cross-validation. Results may provide a preliminary valuable guidance for improving the potency of the analogues and continuing search for potent anti- mycobacterial prior to synthesis.

Keywords: QSAR, anti- mycobacterial, Tuberculosis, Epidemiology, Synthesis, lipophilicity.

INTRODUCTION

Tuberculosis - History

Tuberculosis a “White plague” is an ancient disease presumed that the genus Mycobacterium originated more than 150 million years ago; still remain major problem worldwide. It is a second leading cause of death from infectious disease. In the beginning of 19th century perception of tuberculosis pathogenesis has begun with the work of Theophile Laennec. In 1865, Jean-Antoine villemin have demonstrated the transmissibility of *Mycobacterium tuberculosis* and real fight of humankind started in 1882 when Robert Koch identified these deadly bacteria (Daniel, 2006). *Mycobacterium tuberculosis* has been present in the human population before the beginning of recorded history and has left its mark on all facets of human life. Skeletal of tubercular has been found in the spines of mummies from 3000-2400 BC (Zink, 2003). In the past, TB has been called consumption, because it seemed to consume people with a bloody cough, fever, pallor, and long relentless wasting. Milary tuberculosis is now commonly known as disseminated TB; when the infection invades the circulatory system resulting in lesions which have the appearance of millet seeds on X-ray (Goldman, 2006). As matter of fact the world was not so much excited about the scientific brilliance of Koch‟s discovery of *M. tuberculosis* in 1882, but the accompanying certainty that now the fight against humanity‟s deadliest enemy could really begin. Emerging drug-resistant strains of the disease are presenting a new challenge in the battle to control and prevent tuberculosis. Despite the drugs available today, tuberculosis is still a problem in many nations. Paralleling these advances in the scientific treatment of tuberculosis, the disease has long been the focus of folk medicines. In spite of chemotherapy available today, Mtb still presents problem in developing and developed countries. In 2016, an estimated 8.6 million people developed TB and 1.3 million died from the disease (including 320 000 deaths among HIV-positive people) (Global Tuberculosis Report, 2016).

According to World Health Organization (WHO) estimates, each year, 8 million people worldwide develop active tuberculosis and nearly 2 million die. The WHO also estimates that 36 million people will die of tuberculosis by 2020 if it is not controlled.

Epidemiology

Roughly one-third of the world's population has been infected with *M. tuberculosis*, and it is the second most common cause of death from infectious disease (after HIV) (Dolin, 2010). In 2007 there were an estimated 13.7 million chronic active cases (Global tuberculosis report, 2015) and in 2010 there were 8.8 million new cases, and 1.45 million deaths, mostly in developing countries, amongst them 0.35 million of these deaths occur in those co-infected with HIV. The distribution of tuberculosis is not uniform across the globe; about 80% of the population in many Asian and African countries test positive in tuberculin tests, while only 5–10% of the U.S. population test positive (Kumar, 2007) to tuberculin test.

ligands.

2. Experimental Work

Melting points of all synthesized compounds were determined in open capillaries in microprocessor based melting point apparatus on model VMP-D (VEEGO make) and are uncorrected. Infrared spectra were recorded in KBr using FT-IR 8400S Shimadzu Fourier Transform spectrophotometer. Proton Nuclear Magnetic Resonance spectra were taken on Bruker Avance 400 spectrophotometer at 400 MHz and the chemical shifts are given as parts per million (ppm) downfield from tetramethylsilane (TMS) as internal standard. Mass spectra were recorded on Perkin-Elmer LC-MS PE Sciex API/65. Thin layer chromatography was performed on ready-made Aluminum backed TLC silica Gel GF254 plates as well as on microscopic slides (2x7.5 cm) coated with silica gel G and spots were visualized by exposure to iodine vapors and UV radiation. All solvents used were of AR grade and purchased from SD Fine Chemicals (Ahmedabad); Spectrochem (Mumbai); Finar (Ahmedanad); Loba (Mumbai) and Sigma Aldrich (USA).

General procedure for synthesis of 2-cyano-*N*-(substitutedphenyl) acetamide (147)

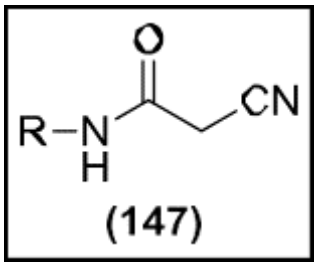

(147)

Synthesis of 2-cyano-*N*-(4-methoxyphenyl) acetamide (147a)

In 100 mL RBF, 4-Methoxy aniline (0.044 mol, 5.77 g) was carefully added to ethyl cyanoacetate (0.044 mol, 5 g) in dimethylformamide (7 mL) and refluxed for 6-8 h. The reaction mixture was allowed to cool to obtain solid. The solid obtained was filtered and dried. The crude product was recrystallized from ethanol to yield colourless crystalline compound.

Synthesis of *N*-(4-chlorophenyl)-2-cyanoacetamide (147b)

The compound was synthesized using essentially the same procedure as described for compound **(147a)**, and some non-critical variations.

Synthesis of 2-cyano-*N*-(2,4-dimethylphenyl) acetamide (147c).

The compound was synthesized using essentially the same procedure as described for compound **(147a)**, and some non-critical variations.

Synthesis of 2-cyano-phenylacetamide (147d)

The compound was synthesized using essentially the same procedure as described for compound **(147a)**, and some non-critical variations.

Synthesis of 2-cyano-*N*-(*p*-tolyl) acetamide (147e)

The compound was synthesized using essentially the same procedure as described for compound **(147a)**, and some non-critical variations.

Molecular formula	C10H10N2O
Molecular weight	174.08 gm/mol
% yield	85.42%
Melting point	180-184 °C (183-185 °C) (Markovic, 1996)
TLC (Mobile Phase)	n-Hexane: Ethyl acetate: 50:50
Rf value	0.57

Synthesis of 2-cyano-*N*-(4-fluorophenyl) acetamide (147f)

The compound was synthesized using essentially the same procedure as described for compound **(147a)**, and some non-critical variations.

Molecular formula	C9H7FN2O
Molecular weight	178.05 gm/mol
% yield	78.38%
Melting point	135-139 °C
TLC (Mobile Phase)	n-Hexane : Ethyl acetate : 50:50
Rf value	0.41

Synthesis of *N*-(3-chloro-4-fluorophenyl)-2-cyanoacetamide (147g)

The compound was synthesized using essentially the same procedure as described for compound **(147a)**, and some non-critical variations.

Synthesis of 2-cyano-*N*-(2,3-dimethylphenyl) acetamide (147h)

The compound was synthesized using essentially the same procedure as described for compound **(147a)**, and some non-critical variations.

Molecular formula	C11H12N2O
Molecular weight	188.09 gm/mol
% yield	74.87%
Melting point	141-144 °C (147-149 °C) (Purkayastha, 1993)
TLC (Mobile Phase)	n-Hexane: Ethyl acetate: 50:50
Rf value	0.48

Synthesis of 2-cyano-*N*-(*o*-tolyl) acetamide (147i)

The compound was synthesized using essentially the same procedure as described for compound **(147a)**, and some non-critical variations.

Synthesis of *N*-(3-chlorophenyl)-2-cyanoacetamide (147j)

The compound was synthesized using essentially the same procedure as described for compound **(147a)**, and some non-critical variations.

Synthesis of 2-cyanoacetamide (147k)

In 500 mL RBF, concentrated aqueous ammonia (0.044 mol, 0.749 ml) was mixed carefully with ethyl cyanoacetate (0.044 mol, 5 g) at 0-5°C. Reaction mixture turned cloudy with exotherm within 3 min after addition. Keep loosely stoppered flask at 0°C for 1 h. filter the crystals and wash it with ice-cold ethanol. Dry the product in air and recrystallized from ethanol to obtain white coloured compound (Gadani, 2013).

Synthesis of 2-cyano-*N*-(2,3-dichlorophenyl) acetamide (147l)

The compound was synthesized using essentially the same procedure as described for compound **(147a)**, and some non-critical variations.

Synthesis of 2-cyano-*N*-(3,4-dichlorophenyl) acetamide (147m)

The compound was synthesized using essentially the same procedure as described for compound **(147a)**, and some non-critical variations.

Synthesis of 2-cyano-*N*-(2-methoxyphenyl) acetamide (147n)

The compound was synthesized using essentially the same procedure as described for compound **(147a)**, and some non-critical variations.

Synthesis of 2-cyano-*N*-(4-ethoxyphenyl) acetamide (147o)

The compound was synthesized using essentially the same procedure as described for compound **(147a)**, and some non-critical variations.

Synthesis of 2-cyano-*N*-(substituted phenyl)-3,3bis(methylthio) acrylamide (S, S- acetal) (148)

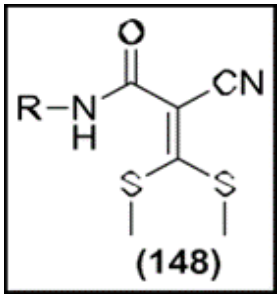

(148)

Synthesis of 2-cyano-*N*-(4-methoxyphenyl)-3,3-bis(methylthio)acrylamide (148a)

To solution of potassium hydroxide (0.0526 mol, 2.95 gm) in 5 mL water, 2-cyano-N- (4- methoxyphenyl) acetamide (0.0263 mol, 5 gm) was added with continuous stirring and cooled at 0-5°C. To above cooled solution 15 mL of DMF was added, and carbon disulphide (0.0312 mol, 2.37 gm) was added dropwise to this reaction mixture. Reaction mixture was allowed to stirr for 30 minutes. To this reaction mixture dimethylsulphate (0.0624 mol, 6.06 gm) was added drop wise over a period of 10 min. The reaction mixture was stirred for 2 h and kept in refrigerator for 12 h and poured in to ice-water mixture. The solid obtained was filtered, washed with water and dried. Recrystallization from ethanol yield colourless crystalline product.

Synthesis of *N*-(4-chlorophenyl) -2-cyano-3,3-bis (methylthio)acrylamide (148b)

The compound was synthesized using essentially the same procedure as described for compound **(148a)**, and some non-critical variations.

Synthesis of 2-cyano-*N*-(2,4-dimethylphenyl)-3,3-bis(methylthio)acrylamide (148c)

The compound was synthesized using essentially the same procedure as described for compound **(148a)**, and some non-critical variations.

7.2.1 Synthesis of 2-cyano-3,3 bis(methylthio)-*N*-phenylacrylamide (148d)

The compound was synthesized using essentially the same procedure as described for compound **(148a)**, and some non-critical variations.

Synthesis of 2-cyano-3,3-bis(methylthio)-*N*-(*p*-tolyl) acrylamide (148e)

The compound was synthesized using essentially the same procedure as described for compound **(148a)**, and some non-critical variations.

Synthesis of 2-cyano-*N*-(4-fluorophenyl)-3,3-bis(methylthio)acrylamide (148f)

The compound was synthesized using essentially the same procedure as described for compound **(148a)**, and some non-critical variations.

Synthesis of *N*-(3-chloro-4-fluorophenyl)-2-cyano-3,3-bis (methylthio) acrylamide (148g)

The compound was synthesized using essentially the same procedure as described for compound **(148a)**, and some non-critical variations.

Molecular formula	C12H10ClFN2OS2
Molecular weight	315.99 gm/mol
% yield	47.9%
Melting point	142-146 °C
TLC (Mobile Phase)	n-Hexane : Ethyl acetate : 50:50
Rf value	0.64

Synthesis of 2-cyano-*N*-(2,3-dimethylphenyl)-3,3-bis(methylthio)acrylamide (148h)

The compound was synthesized using essentially the same procedure as described for compound **(148a)**, and some non-critical variations.

Molecular formula	C14H16N2OS2
Molecular weight	292.07 gm/mol
% yield	75.4%
Melting point	86-89 °C (91-93 °C) (Elgemeie, 1997)
TLC (Mobile Phase)	n-Hexane : Ethyl acetate : 50:50
Rf value	0.67

Synthesis of 2-cyano-3,3-bis(methylthio)-*N*-(*o*-tolyl) acrylamide (148i)

The compound was synthesized using essentially the same procedure as described for compound **(148a)**, and some non-critical variations.

Synthesis of 2-cyano-3,3-bis(methylthio)acrylamide (148k)

The compound was synthesized using essentially the same procedure as described for compound **(148a)**, and some non-critical variations.

Synthesis of *N*-(3-chlorophenyl)-2-cyano-3,3-bis(methylthio)acrylamide (148j)

The compound was synthesized using essentially the same procedure as described for compound **(148a)**, and some non-critical variations.

Synthesis of 2-cyano-*N*-(2,3-dichlorophenyl)-3,3-bis (methylthio) acrylamide (148l)

The compound was synthesized using essentially the same procedure as described for compound **(148a)**, and some non-critical variations.

Molecular formula	C12H10Cl2N2OS2
Molecular weight	331.96 gm/mol
% yield	57.28%
Melting point	110-112 °C (113-116 °C)
TLC (Mobile Phase)	n-Hexane : Ethyl acetate : 50:50
Rf value	0.59

Synthesis of 2-cyano-*N*-(3,4-dichlorophenyl)-3,3-bis(methylthio)acrylamide (148m)

The compound was synthesized using essentially the same procedure as described for compound **(148a)**, and some non-critical variations.

Molecular formula	C12H10Cl2N2S2O
Molecular weight	331.96 gm/mol
% yield	62.59%
Melting point	116-118 °C (119-122 °C) (Elgemeie, 1997)
TLC (Mobile Phase)	n-Hexane : Ethyl acetate : 50:50
Rf value	0.47

Synthesis of 2-cyano-*N*-(2-methoxyphenyl)-3,3-bis(methylthio)acrylamide (148n)

The compound was synthesized using essentially the same procedure as described for compound **(148a)**, and some non-critical variations.

Synthesis of 2-cyano-*N*-(4-ethoxyphenyl)-3,3-bis(methylthio)acrylamide (148o)

The compound was synthesized using essentially the same procedure as described for compound **(148a)**, and some non-critical variations.

Molecular formula	C13H14N2O2S2
Molecular weight	294.39 gm/mol
% yield	37.42%
Melting point	110-112 °C
TLC (Mobile Phase)	n-Hexane : Ethyl acetate : 50:50
Rf value	0.48

Synthesis of 2-cyano-*N*-(substituted phenyl)-3-(methylthio)-3-[(substituted) amino] acrylate (S, N-acetals) (149)

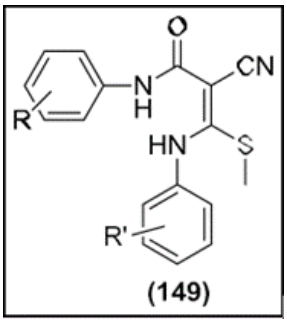

(149)

Synthesis of 2-cyano-*N*-(4-methoxyphenyl)-3-((4-methoxyphenyl) amino)-3-(methylthio)acrylamide (149a)

2-Cyano-*N*-(4-methoxyphenyl)-3,3 bis(methylthio)acrylamide (0.0169 mol, 5 gm) was dissolved in 30 mL of isopropyl alcohol. *p*-Anisidine (0.0169 mol, 2.08 gm) was added and mixture was refluxed for 15 h. After completion of reaction, reaction mixture was poured into ice cold water. Solid obtained was filtered and dried. Recrystallization from toluene yielded colourless crystalline product.

Synthesis of 3-((4-chlorophenyl) amino)-2-cyano-*N*-(4-methoxyphenyl) -3- (methylthio)acrylamide (149b)

The compound was synthesized using essentially the same procedure as described for compound **(149a)**, and some non-critical variations.

Synthesis of 2-cyano-3-((2,3-dimethylphenyl) amino)-*N*-(4-methoxyphenyl)-3-(methylthio)acrylamide (149c)

The compound was synthesized using essentially the same procedure as described for compound **(149a)**, and some non-critical variations.

Synthesis of 2-cyano-*N*-(4-methoxyphenyl)-3-(methylthio)-3- (phenylamino) acrylamide (149d)

The compound was synthesized using essentially the same procedure as described for compound **(149a)**, and some non-critical variations.

Synthesis of 2-cyano-*N*-(4-methoxyphenyl)-3-(methylthio)-3- morpholinoacrylamide (149e)

The compound was synthesized using essentially the same procedure as described for compound **(149a)**, and some non-critical variations.

Molecular formula	C16H19N3O3S
Molecular weight	333.41 gm/mol
% yield	86.42%
Melting point	142-145 °C
TLC (Mobile Phase)	n-Hexane : Ethyl acetate : 50:50
Rf value	0.18

Synthesis of 2-cyano-3-(methylthio)-3-(phenylamino)-*N*-(p-tolyl) acrylamide (149f)

The compound was synthesized using essentially the same procedure as described for compound **(149a)**, and some non-critical variations.

Molecular formula	C18H17N3OS
Molecular weight	323.11 gm/mol
% yield	68.22%
Melting point	113-115 °C
TLC (Mobile Phase)	n-Hexane : Ethyl acetate : 50:50
Rf value	0.69

Synthesis of 3-((4-chlorophenyl) amino)-2-cyano-3-(methylthio)-*N*-(p- tolyl) acrylamide (149g)

The compound was synthesized using essentially the same procedure as described for compound **(149a)**, and some non-critical variations.

Molecular formula	C18H16ClN3OS
Molecular weight	357.07 gm/mol
% yield	84.24%
Melting point	156-161 °C (157-159 °C) (Shahak, 1973)
TLC (Mobile Phase)	n-Hexane : Ethyl acetate : 50:50
Rf value	0.71

Synthesis of 2-cyano-3-((3,4-dichlorophenyl) amino)-3-(methylthio)-*N*- phenylacrylamide (149h)

The compound was synthesized using essentially the same procedure as described for compound **(149a)**, and some non-critical variations.

Molecular formula	C11H9 Cl2N3OS
Molecular weight	302.18 gm/mol
% yield	49.12%
Melting point	180-182 °C (178-181 °C) (Gadani, 2013)
TLC (Mobile Phase)	n-Hexane : Ethyl acetate : 50:50
Rf value	0.33

Synthesis of 2-cyano-3-((2,4-dimethylphenyl) amino)-N-(4-ethoxyphenyl)-3-(methylthio)acrylamide (149i)

The compound was synthesized using essentially the same procedure as described for compound **(149a)**, and some non-critical variations.

Molecular formula	C21H23N3O2S
Molecular weight	381.49 gm/mol
% yield	51.12%
Melting point	130-133 °C
TLC (Mobile Phase)	n-Hexane : Ethyl acetate : 50:50
Rf value	0.69

Synthesis of *N*-(4-chlorophenyl)-2-cyano-3-((2,4-dimethylphenyl) amino)-3-(methylthio)acrylamide (149j)

The compound was synthesized using essentially the same procedure as described for compound **(149a)**, and some non-critical variations.

Synthesis of 2-cyano-N-(2,4-dimethylphenyl)-3-((4-methoxyphenyl) amino)- 3-(methylthio)acrylamide (149k)

The compound was synthesized using essentially the same procedure as described for compound (149a), and some non-critical variations.

Molecular formula	C20H21N3O2S
Molecular weight	367.46 gm/mol
% yield	68.41%
Melting point	116-119 °C (112-114 °C) (Dieter, 1981)
TLC (Mobile Phase)	n-Hexane : Ethyl acetate : 50:50
Rf value	0.67

Synthesis of 2-cyano-3-((3,4-dichlorophenyl) amino)-N-(2,3- dimethylphenyl)-3-(methylthio)acrylamide (149l)

The compound was synthesized using essentially the same procedure as described for compound (149a), and some non-critical variations.

Molecular formula	C19H17Cl2N3OS
Molecular weight	406.33 gm/mol
% yield	74.44%
Melting point	120-124 °C (122-123 °C) (Dieter, 1981)
TLC (Mobile Phase)	n-Hexane : Ethyl acetate : 50:50
Rf value	0.73

Synthesis of 2-cyano-3-((2,4-dimethylphenyl) amino)-N-(4-fluorophenyl)-3-(methylthio)acrylamide (149m)

The compound was synthesized using essentially the same procedure as described for compound (149a), and some non-critical variations.

Molecular formula	C19H18FN3OS
Molecular weight	355.43 gm/mol
% yield	76.86%
Melting point	121-123 °C (116-118 °C) (Dieter, 1981)
TLC (Mobile Phase)	n-Hexane : Ethyl acetate : 50:50
Rf value	0.72

Synthesis of 5-amino-N-substituted phenyl-3-(substituted phenylamino)- 1H- pyrazole-4-carboxamide (150)

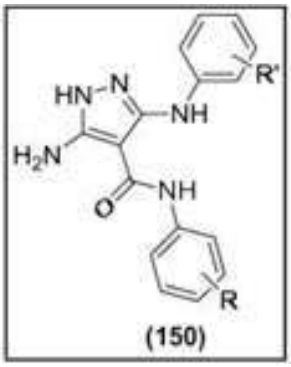

(150)

Synthesis of 5-amino-N-(4-methoxyphenyl)-3-((4-methoxyphenyl) amino)- 1H- pyrazole-4-carboxamide (150a)

The solution of 2-cyano-N-(4-methoxyphenyl)-3-((4-methoxyphenyl) amino)-3- (methylthio)acrylamide (0.0108 mol, 4 gm) in 20 mL ethanol was refluxed with hydrazine hydrate (99%, 0.0108 mol, 0.35 gm) for 3-4 hours. Completion of reaction was monitored by TLC. Ethanol was distilled off. Obtained solid was filtered and dried. Recrystallization from ethanol yielded crystalline product which is characterized as 5- amino-N- (4-methoxyphenyl)- 3-((4-methoxyphenyl) amino) -1H-pyrazole-4-carboxamide (150a).

Molecular formula	C18H19N5O3
Molecular weight	353.38 gm/mol
% yield	79.24%
Melting point	203-206 °C

TLC (Mobile Phase)	n-Hexane : Ethyl acetate : 10:90
Rf value	0.45
IR (KBr, cm^{-1})	3367 & 3078 (NH2 str.), 1660 (-CO-NH str.), 1249 (C-N str.), 1033 (C-O-C)
MASS (m/e)	354.4 (M+1)
^{1}H NMR (DMSO-d6, δppm)	δ 11.1(s, 1H, NH-Ph., D2O exchangeable), δ 8.6(s, 1H, CONH-Ph., D2O exchangeable), δ 8.4(s, 1H, NH-Pyrazole., D2O exchangeable), δ 6.7- 7.4 (m, 8H, Ph-H), δ 5.9(s, 2H,-NH2- Pyrazole, D2O exchangeable), δ 3.6-3.7(d, 6H, Ph-OCH3)

Synthesis of 5-amino-3-((4-chlorophenyl)amino)-*N*-(4-methoxyphenyl)-1*H*- pyrazole-4-carboxamide (150b)

The compound was synthesized using essentially the same procedure as described for compound **(150a)**, and some non-critical variations.

Molecular formula	C17H16ClN5O2
Molecular weight	357.79 gm/mol
% yield	59.29%
Melting point	226-230 °C
TLC (Mobile Phase)	n-Hexane : Ethyl acetate : 10:90
Rf value	0.65
IR (KBr, cm^{-1})	3357 & 3051 (NH2 str.), 1647 (-CO-NH str.), 1249 (C-N str.),1033 (C-O-C)
MASS (m/e)	358 (M+1), 360 (M+2)
^{1}H NMR (DMSO-d6, δppm)	δ 11.3(s, 1H, NH-Ph., D2O exchangeable), δ 8.8(s, 1H, CONH-Ph., D2O exchangeable), δ 8.5(s, 1H, NH-Pyrazole, D2O exchangeable),
	δ 6.8- 7.4 (m, 8H, Ph-H), δ 6.03(s, 2H,-NH2- Pyrazole, D2O exchangeable), δ 3.7(s, 3H, Ph- OCH3)

Synthesis of 5-amino-3-((2,3-dimethylphenyl) amino)-*N*-(4- methoxyphenyl) -1*H*- pyrazole-4-carboxamide (150c)

The compound was synthesized using essentially the same procedure as described for compound **(150a)**, and some non-critical variations.

Molecular formula	C19H21N5O2
Molecular weight	351.40 gm/mol
% yield	68.41%
Melting point	158-160 °C
TLC (Mobile Phase)	n-Hexane : Ethyl acetate : 10:90
Rf value	0.59
IR (KBr, cm^{-1})	3357 & 3149 (NH2 str.), 1610 (-CO-NH str.), 1255 (C-N str.),1035 (C-O-C)
MASS (m/e)	351.4 (M)
^{1}H NMR (DMSO-d6, δppm)	δ 11.3(s, 1H, NH-Ph., D2O exchangeable), δ 8.8(s, 1H, CONH-Ph., D2O exchangeable), δ 8.5(s, 1H, NH-Pyrazole, D2O exchangeable), δ 6.8- 7.4 (m, 7H, Ph-H), δ 6.03(s, 2H,-NH2- Pyrazole, D2O exchangeable), δ 3.7(s, 3H, Ph- OCH3), δ 2.5(s, 6H, Ph-CH3)

Synthesis of 5-amino-*N*-(4-methoxyphenyl)-3-(phenylamino)-1*H*-pyrazole- 4- carboxamide (150d)

The compound was synthesized using essentially the same procedure as described for compound **(150a)**, and some non-critical variations.

Molecular formula	C17H17N5O2
Molecular weight	323.35 gm/mol
% yield	74.44%
Melting point	165-170 °C
TLC (Mobile Phase)	n-Hexane : Ethyl acetate : 10:90
Rf value	0.68
IR (KBr, cm^{-1})	3352 & 3105 (NH2 str.), 1654 (-CO-NH str.)
MASS (m/e)	324.5 (M+1)
^{1}H NMR (DMSO-d6, δppm)	δ 11.3(s, 1H, NH-Ph, D2O exchangeable), δ 8.8(s, 1H, CONH-Ph, D2O exchangeable), δ 8.5(s, 1H, NH-Pyrazole, D2O exchangeable), δ 6.8- 7.4 (m, 9H, Ph-H), δ 6.03(s, 2H,-NH2- Pyrazole, D2O exchangeable), δ 3.7(s, 3H, Ph-OCH3)

Synthesis of 5-amino-*N*-(4-methoxyphenyl)-3-morpholino-1*H*-pyrazole-4- carboxamide (150e)

The compound was synthesized using essentially the same procedure as described for compound **(150a)**, and some non-critical variations.

Molecular formula	C15H19N5O3
Molecular weight	317.34 gm/mol
% yield	76.86%
Melting point	162-164 °C
TLC (Mobile Phase)	n-Hexane : Ethyl acetate : 10:90
Rf value	0.36
IR (KBr, cm^{-1})	3421 & 3110 (NH2 str.), 1658 (-CO-NH str.), 1234 (C-N str.), 1033 (C-O-C)
MASS (m/e)	318.2 (M+1)
^{1}H NMR (DMSO-d6, δppm)	δ 11.3(s, 1H, NH-Ph, D2O exchangeable), δ 8.8(s, 1H, CONH-Ph, D2O exchangeable), δ 6.8- 7.4 (m, 4H,-CH-Ph), δ 6.03(s, 2H,-NH2- Pyrazole, D2O exchangeable), δ 3.7(s, 3H, Ph- OCH3), δ 3.3-3.5(m, 8H, Morpholine)

Synthesis of 5-amino-3-(phenylamino)-*N*-(*p*-tolyl)-1*H*-pyrazole-4- carboxamide (150f)

The compound was synthesized using essentially the same procedure as described for compound **(150a)**, and some non-critical variations.

Molecular formula	C17H17N5O
Molecular weight	307.35 gm/mol
% yield	82.86%
Melting point	208-212 °C
TLC (Mobile Phase)	n-Hexane : Ethyl acetate : 10:90
Rf value	0.56
IR (KBr, cm^{-1})	3367 & 3077 (NH2 str.), 1637 (-CO-NH str.),
	1238 (C-N str.)
MASS (m/e)	308.5 (M+1)

^{1}H NMR (DMSO-d6, δppm)	δ 11.3(s, 1H, NH-Ph, D2O exchangeable), δ 8.7(s, 1H, CONH-Ph, D2O exchangeable), δ 8.6(s, 1H, NH-Pyrazole, D2O exchangeable), δ 7.08- 7.4 (m, 9H, Ph-H), δ 6.04(s, 2H,-NH2-Pyrazole, D2O exchangeable), δ 2.2(s, 3H, Ph-CH3)

Synthesis of 5-amino-3-((4-chlorophenyl) amino)-*N*-(*p*-tolyl)-1*H*-pyrazole-4- carboxamide (150g)

The compound was synthesized using essentially the same procedure as described for compound **(150a)**, and some non-critical variations.

Molecular formula	C17H16ClN5O
Molecular weight	341.79 gm/mol
% yield	51.42%
Melting point	254-256 °C
TLC (Mobile Phase)	n-Hexane : Ethyl acetate : 10:90
Rf value	0.65
IR (KBr, cm^{-1})	3357 & 3133 (NH2 str.), 1637 (-CO-NH str.), 1242 (C-N str.)
MASS (m/e)	342.9 (M+1), 344.3 (M+2)
^{1}H NMR (DMSO-d6, δppm)	δ 11.3(s, 1H, NH-Ph, D2O exchangeable), δ 8.7(s, 1H, CONH-Ph, D2O exchangeable), δ 8.6(s, 1H, NH-Pyrazole, D2O exchangeable), δ 7.08- 7.4 (m, 8H, Ph-H), δ 6.04(s, 2H,-NH2-Pyrazole, D2O exchangeable), δ 2.2(s, 3H, Ph-CH3)

Synthesis 5-amino-3-((3,4-dichlorophenyl)amino)-1*H*-pyrazole-4- carboxamide (150h)

The compound was synthesized using essentially the same procedure as described for compound **(150a)**, and some non-critical variations.

Molecular formula	C10H9Cl2N5O
Molecular weight	282.12 gm/mol
% yield	72.42%
Melting point	255-258 °C
TLC (Mobile Phase)	n-Hexane : Ethyl acetate : 10:90
Rf value	0.71
IR (KBr, cm^{-1})	3359 & 3001 (NH2 str.), 1614 (-CO-NH str.), 1232 (C-N str.)
MASS (m/e)	283.1 (M+1), 285.4 (M+2), 287.9 (M+4)
^{1}H NMR (DMSO-d6, δppm)	δ 11.1(s, 1H, NH-Ph, D2O exchangeable), δ 9.6(s, 2H, CONH2-Ph, D2O exchangeable), δ 8.6(s, 1H, NH-Pyrazole, D2O exchangeable), δ 6.8-7.8(m, 3H, Ph-H),δ 5.9(s, 2H,-NH2-Pyrazole, D2O exchangeable)

Synthesis of 5-amino-3-((2,4-dimethylphenyl) amino)-*N*-(4-ethoxyphenyl)-1*H*- pyrazole-4-carboxamide (150i)

The compound was synthesized using essentially the same procedure as described for compound **(150a)**, and some non-critical variations.

Molecular formula	C20H22N5O2
Molecular weight	365.43 gm/mol
% yield	69.12%
Melting point	181-183 °C
TLC (Mobile Phase)	n-Hexane : Ethyl acetate : 10:90
Rf value	0.59
IR (KBr, cm^{-1})	3409 & 3324 (NH2 str.), 1652 (-CO-NH str.)
MASS (m/e)	366.9 (M+1)
^{1}H NMR (DMSO-d6, δppm)	δ 11.1(s, 1H, NH-Ph, D2O exchangeable), δ 9.9(s, 1H, CONH-Ph, D2O exchangeable), δ 9.6(s, 1H, NH-Pyrazole, D2O exchangeable), δ 6.08- 8.8 (m, 7H, Ph-H), δ 5.9(s, 2H,-NH2-Pyrazole, D2O exchangeable), δ 1.8(s, 6H, Ph- CH3), δ 1.3-1.7(s, 5H-Ar, -OCH2CH3)

Synthesis of 5-amino-*N*-(4-chlorophenyl)-3-((2,4-dimethylphenyl) amino)- 1*H*- pyrazole-4-carboxamide (150j)

The compound was synthesized using essentially the same procedure as described for compound **(150a)**, and some non-critical variations.

Molecular formula	C18H18ClN5O
Molecular weight	355.82 gm/mol
% yield	72.7%
Melting point	210-214 °C
TLC (Mobile Phase)	n-Hexane : Ethyl acetate : 10:90
Rf value	0.59
IR (KBr, cm^{-1})	3319 & 3107 (NH2 str.), 1647 (-CO-NH str.), 1242 (C-N str.)
MASS (m/e)	356.9 (M+1), 358.2 (M+2)
^{1}H NMR (DMSO-d6, δppm)	δ 11.2(s, 1H, NH-Ph, D2O exchangeable), δ 8.8(s, 1H, CONH-Ph, D2O exchangeable), δ 8.5(s, 1H, NH-Pyrazole, D2O exchangeable), δ 6.8- 7.4 (m, 7H, Ph-H), δ 6.04(s, 2H,-NH2-Pyrazole, D2O exchangeable), δ 2.2-2.1(s, 6H, Ph-CH3)

Synthesis of 5-amino-*N*-(2,4-dimethylphenyl)-3-((4-methoxyphenyl) amino)-1*H*- pyrazole-4-carboxamide (150k)

The compound was synthesized using essentially the same procedure as described for compound **(150a)**, and some non-critical variations.

Synthesis of 5-amino-3-((3,4-dichlorophenyl) amino)-*N*-(2,3- dimethylphenyl)-1*H*- pyrazole-4-carboxamide (150l)

The compound was synthesized using essentially the same procedure as described for compound **(150a)**, and some non-critical variations.

Molecular formula	C18H17Cl2N5O
Molecular weight	390.27 gm/mol
% yield	82.8%
Melting point	242-245 °C
TLC (Mobile Phase)	n-Hexane : Ethyl acetate : 10:90
Rf value	0.69
IR (KBr, cm^{-1})	3367 & 3276 (NH2 str.), 1639 (-CO-NH str.), 1247 (C-N str.)
MASS (m/e)	391.4 (M+1), 393.0 (M+2)

	395.8 (M+4)
^{1}H NMR (DMSO-d6, δppm)	δ 11.2(s, 1H, NH-Ph, D2O exchangeable), δ 9.0(s, 1H, CONH-Ph, D2O exchangeable), δ 8.6(s, 1H, NH-Pyrazole, D2O exchangeable), δ 6.9- 7.7(m, 6H, Ph-H), δ 6.01(s, 2H,-NH2-Pyrazole, D2O exchangeable), δ 2.0-2.2(s, 6H, Ph-CH3)

Synthesis of 5-amino-3-((2,4-dimethylphenyl) amino)-*N*-(4-fluorophenyl)- 1*H*- pyrazole-4-carboxamide (150m)

The compound was synthesized using essentially the same procedure as described for compound **(150a)**, and some non-critical variations.

Synthesis of 5-amino-*N*-(2-methoxyphenyl)-3-(*m*-tolylamino)-1*H*- pyrazole-4-carboxamide (150n)

The compound was synthesized using essentially the same procedure as described for compound **(150a)**, and some non-critical variations.

Synthesis of 5-amino-3-((4-chlorophenyl) amino)-1*H*-pyrazole-4- carboxamide (150o)

The compound was synthesized using essentially the same procedure as described for compound **(150a)**, and some non-critical variations.

Synthesis of 5-amino-3-((3,4-difluorophenyl) amino)-*N*-(4-fluorophenyl)- 1*H*- pyrazole-4-carboxamide (150p)

The compound was synthesized using essentially the same procedure as described for compound **(150a)**, and some non-critical variations.

Synthesis of 5-amino-*N*-(4-ethoxyphenyl)-3-(phenylamino)-1*H*-pyrazole- 4- carboxamide (150q)

The compound was synthesized using essentially the same procedure as described for compound **(150a)**, and some non-critical variations.

Synthesis of 5-amino-*N*-(2,3-dichlorophenyl)-3-(4-ethylpiperazin-1-yl)-1*H*- pyrazole-4-carboxamide (150r)

The compound was synthesized using essentially the same procedure as described for compound **(150a)**, and some non-critical variations.

Synthesis of 5-amino-*N*-(3,4-dichlorophenyl)-3-(pyrrolidin-1-yl)-1*H*- pyrazole-4- carboxamide (150s)

The compound was synthesized using essentially the same procedure as described for compound **(150a)**, and some non-critical variations.

Synthesis of 5-amino-*N*-phenyl-3-(phenylamino)-1*H*-pyrazole-4- carboxamide (150t)

The compound was synthesized using essentially the same procedure as described for compound **(150a)**, and some non-critical variations.

Synthesis of 5-amino-*N*-phenyl-3-(*p*-tolylamino)-1*H*-pyrazole-4- carboxamide (150u)

The compound was synthesized using essentially the same procedure as described for compound **(150a)**, and some non-critical variations.

Synthesis of 5-amino-3-((4-chlorophenyl) amino)-*N*-phenyl-1*H*-pyrazole-4- carboxamide (150v)

The compound was synthesized using essentially the same procedure as described for compound **(150a)**, and some non-critical variations.

Synthesis of 5-amino-*N*-(3-chloro-4-fluorophenyl)-3-(*p*-tolylamino)-1*H*- pyrazole- 4-carboxamide (150w)

The compound was synthesized using essentially the same procedure as described for compound **(150a)**, and some non-critical variations.

Synthesis of 5-amino-*N*-(3-chloro-4-fluorophenyl)-3-((4-methoxyphenyl) amino)- 1*H*-pyrazole-4-carboxamide (150x)

The compound was synthesized using essentially the same procedure as described for compound **(150a)**, and some non-critical variations.

Synthesis of 5-amino-*N*-(3-chlorophenyl)-3-((4-fluorophenyl) amino)-1*H*- pyrazole- 4-carboxamide (150y)

The compound was synthesized using essentially the same procedure as described for compound **(150a)**, and some non-critical variations.

Synthesis of 5-amino-*N*-(3-chlorophenyl)-3-((2,3-dimethylphenyl) amino)- 1*H*- pyrazole-4-carboxamide (150z)

The compound was synthesized using essentially the same procedure as described for compound **(150a)**, and some non-critical variations.

Synthesis of 7-hydroxy-5-methyl-*N*-substituted phenyl-2-(substituted phenylamino) pyrazolo[1,5-*a*] pyrimidine-3-carboxamide (151)

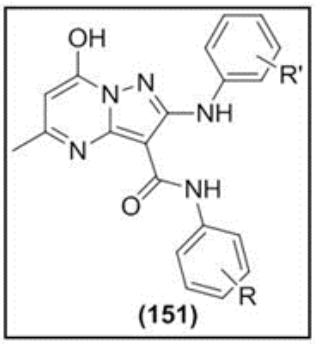

(151)

Synthesis of 7-hydroxy-*N*-(4-methoxyphenyl)-2-((4-methoxyphenyl) amino)- 5-methylpyrazolo[1,5-*a*] pyrimidine-3-carboxamide (151a)

A mixture of 5-amino-*N*-(4-methoxyphenyl)-3-((4-methoxyphenyl) amino)-1*H*- pyrazole-4-carboxamide (0.00566 mol, 2 gm) and ethyl aceto acetate (0.00566 mol, 0.73 gm) was refluxed in oil bath for 1 hour. The reaction was monitored by TLC. After completion, the reaction was poured into ice cold water. Solid obtained was filtered. Recrystallization from chloroform yielded pure crystalline product.

Synthesis of 7-hydroxy-*N*-(4-methoxyphenyl)-5-methyl-2- (phenylamino) pyrazolo[1,5-*a*] pyrimidine-3-carboxamide (151d)

The compound was synthesized using essentially the same procedure as described for compound **(151a)**, and some non-critical variations.

Synthesis of 7-hydroxy-*N*-(4-methoxyphenyl)-5-methyl-2- morpholinopyrazolo[1,5-*a*] pyrimidine-3-carboxamide (151e)

The compound was synthesized using essentially the same procedure as described for compound **(151a)**, and some non-critical variations.

Synthesis of 7-hydroxy-5-methyl-2-(phenylamino)-*N*-(*p*-tolyl) pyrazolo [1,5- *a*] pyrimidine-3-carboxamide (148f)

The compound was synthesized using essentially the same procedure as described for compound **(151a)**, and some non-critical variations.

Synthesis of 2-((4-chlorophenyl) amino)-7-hydroxy-5-methyl-*N*-(*p*- tolyl) pyrazolo[1,5-*a*] pyrimidine-3-carboxamide (151g)

The compound was synthesized using essentially the same procedure as described for compound **(151a)**, and some non-critical variations.

Synthesis of 2-((3,4-dichlorophenyl) amino)-7-hydroxy-5-methylpyrazolo [1,5-*a*] pyrimidine-3-carboxamide (151h)

The compound was synthesized using essentially the same procedure as described for compound **(151a)**, and some non-critical variations.

Synthesis of 2-((2,4-dimethylphenyl)amino)-*N*-(4-ethoxyphenyl)-7-hydroxy- 5- methylpyrazolo[1,5-*a*]pyrimidine-3-carboxamide (151i)

The compound was synthesized using essentially the same procedure as described for compound **(151a)**, and some non-critical variations.

Synthesis of *N*-(4-chlorophenyl)-2-((2,4-dimethylphenyl) amino)-7-hydroxy- 5-methylpyrazolo[1,5-*a*] pyrimidine-3-carboxamide (151j)

The compound was synthesized using essentially the same procedure as described for compound **(151a)**, and some non-critical variations.

Synthesis of *N*-(2,4-dimethylphenyl)-7-hydroxy-2-((4-methoxyphenyl) amino)-5-methylpyrazolo[1,5-*a*] pyrimidine-3-carboxamide (151k)

The compound was synthesized using essentially the same procedure as described for compound **(151a)**, and some non-critical variations.

Synthesis of 2-((3,4-difluorophenyl) amino)-*N*-(4-fluorophenyl)-7-hydroxy- 5- methylpyrazolo[1,5-*a*] pyrimidine-3-carboxamide (151p)

The compound was synthesized using essentially the same procedure as described for compound **(151a)**, and some non-critical variations.

Synthesis of *N*-(4-ethoxyphenyl)-7-hydroxy-5-methyl-2-(phenylamino) pyrazolo[1,5-*a*] pyrimidine-3-carboxamide (151q)

The compound was synthesized using essentially the same procedure as described for compound **(151a)**, and some non-critical variations.

Synthesis of *N*-(2,3-dichlorophenyl)-2-(4-ethylpiperazin-1-yl)-7-hydroxy-5-methylpyrazolo[1,5-*a*] pyrimidine-3-carboxamide (151r)

The compound was synthesized using essentially the same procedure as described for compound **(151a)**, and some non-critical variations.

Synthesis of *N*-(3,4-dichlorophenyl)-7-hydroxy-5-methyl-2-(pyrrolidin-1- yl) pyrazolo[1,5-*a*]pyrimidine-3-carboxamide (151s)

The compound was synthesized using essentially the same procedure as described for compound **(151a)**, and some non-critical variations.

Synthesis of 7-hydroxy-5-methyl-*N*-phenyl-2-(phenylamino) pyrazolo [1,5- *a*]pyrimidine-3-carboxamide (151t)

The compound was synthesized using essentially the same procedure as described for compound **(151a)**, and some non-critical variations.

Synthesis of 7-hydroxy-5-methyl-*N*-phenyl-2-(*p*-tolylamino) pyrazolo [1,5- *a*] pyrimidine-3-carboxamide (151u)

The compound was synthesized using essentially the same procedure as described for compound **(151a)**, and some non-critical variations.

Synthesis of 2-((4-chlorophenyl) amino)-7-hydroxy-5-methyl-*N*- phenyl pyrazolo[1,5-*a*] pyrimidine-3-carboxamide (151v)

The compound was synthesized using essentially the same procedure as described for compound **(151a)**, and some non-critical variations.

Synthesis of *N*-(3-chloro-4-fluorophenyl)-7-hydroxy-5-methyl-2-(*p*- tolylamino) pyrazolo[1,5-*a*] pyrimidine-3-carboxamide (151w)

The compound was synthesized using essentially the same procedure as described for compound **(151a)**, and some non-critical variations.

Synthesis of *N*-(3-chloro-4-fluorophenyl)-7-hydroxy-2-((4- methoxyphenyl) amino)-5-methylpyrazolo[1,5-*a*] pyrimidine-3-carboxamide (151x)

The compound was synthesized using essentially the same procedure as described for compound **(151a)**, and some non-critical variations.

Synthesis of *N*-(3-chlorophenyl)-2-((4-fluorophenyl) amino)-7-hydroxy-5-methylpyrazolo[1,5-*a*] pyrimidine-3-carboxamide (151y)

The compound was synthesized using essentially the same procedure as described for compound **(151a)**, and some non-critical variations.

Synthesis of *N*-(3-chlorophenyl)-2-((2,3-dimethylphenyl) amino)-7-hydroxy- 5-methylpyrazolo[1,5-*a*] pyrimidine-3-carboxamide (151z)

The compound was synthesized using essentially the same procedure as described for compound **(151a)**, and some non-critical variations.

RESULTS AND DISCUSSION

Atom Based QSAR Study on Series of Pyrazole Derivatives

Atom-based QSAR model, significantly explains the structure–activity relationship, the model generated based on the molecular alignment obtained by pharmacophore generation. Pharmacophore-based QSAR do not consider ligand features beyond the pharmacophore model, such as possible steric clashes with the receptor. This requires consideration of the entire molecular structure; therefore, an atom-based QSAR (Mahesh and Rajanikant 2012) model is more useful in explaining the structure–activity relationship. In atom-based QSAR, a molecule is treated as a set of overlapping van der Waals spheres. Each atom (and hence each sphere) is placed into one of six categories according to a simple set of rules: hydrogen's attached to polar atoms are classified as hydrogen bond donors(D); carbons, halogens, and C–H hydrogen's are classified as hydrophobic/non-polar (H); atoms with an explicit negative ionic charge are classified as negative ionic (N); atoms with an explicit positive ionic charge are classified as positive ionic (P); non-ionic atoms are classified as electron-withdrawing (W); and all other types of atoms are classified as miscellaneous (X). For purposes of QSAR development, van der Waals models of the aligned training set molecules were placed in a regular grid of cubes, with each cube allotted zero or more 'bits' to account for the different types of atoms in the training set that occupy the cube. This representation gives rise to binary-valued occupation patterns that can be used as independent variables to create partial least-squares (PLS) QSAR models. QSAR modelling was carried out by dividing the dataset into training set (70%) and test set (30%) in a random manner.It follows Partial Least Square (PLS), that assumes a linear relationship between feature vector, X, and target property, Y, unlike MLR, PLS is more appropriate when the number of features greatly exceed the number of samples and when features are highly collinear. The atom based QSAR model was performed in Maestro software package (Maestro v10.1, Schrodinger, LLC, NEW YORK).

Figure 1 Outlay for Atom based 3d-QSAR Study

QSAR study on series of 5-amino-N-substituted phenyl-3-(substituted phenylamino)- 1H-pyrazole-4-carboxamide (PM derivatives)

Ligand Preparation

Atom based QSAR study was carried out using Schrödinger (Maestro v10.1, Schrodinger, LLC, NEW YORK) software. All the compounds were sketched using Maestro and geometry optimization was carried out using semi-empirical OPLS_2005 force field. All the molecules were divided into training set and test set. For every compound of the series, the experimental values of biological activity are used in the negative logarithmic scale of pMIC to achieve normal distribution.

Selection of training and test sets

Set of 26 compounds was randomly divided into training set and test set of 19 and 7 compounds respectively. Structure of training and test set molecules are presented in table 33 and table 34 along with their biological activity data.

Table: Biological activity of training set molecule

Com. No.	R	R'	MIC	pMIC
1 (1A)	4-OCH3	4-OCH3	1.6	8.344
2 (1C)	4-OCH3	2,3- di-CH3	50	6.847
3 (1D)	4-OCH3	-H	25	7.112
4 (1E)	4-OCH3	Morpholine	12.5	7.405
5 (1F)	4-CH3	-H	50	6.789
6 (1G)	4-CH3	4-Cl	1.6	8.246
7 (1H)	-NH2	3,4-di-Cl	1.6	8.246
8 (1J)	4-Cl	2,4-di-CH3	50	6.852
9 (1L)	2,3- di-CH3	3,4-di-Cl	25	7.139
10 (1N)	2-OCH3	3-CH3	1.6	8.324
11 (1O)	-NH2	4-Cl	12.5	7.304
12 (1Q)	-OC2H5	3-CH3	6.25	7.732
13 (1S)	2-OCH3	N-Me piperazine	3.12	8.038
14 (1T)	-H	-H	6.25	7.671
15 (1V)	-H	4-Cl	6.25	7.72
16 (1W)	3-Cl 4-F	4-CH3	6.25	7.76
17 (1X)	3-Cl 4-F	4-OCH3	100	6.575
18 (1Y)	3-Cl	4-F	25	7.141
19 (1Z)	3-Cl	2,3- di-CH3	25	7.153

Table: Biological activity of test set molecules

Com. No.	R	R'	MIC	pMIC
1 (1B)	4-OCH3	4-Cl	1.6	8.349
2 (1I)	-OC2H5	2,4- di-CH3	50	6.864
3 (1K)	2,4- di-CH3	4-OCH3	6.25	7.75
4 (1M)	4-F	2,4- di-CH3	12.5	7.434
5 (1P)	4-F	3,4- di-F	1.6	8.337
6 (1R)	2,3- di-Cl	Piperidine	25	7.186
7 (1U)	-H	4-CH3	12.5	7.391

QSAR Modelling

Atom-based QSAR was generated by using grid size of 1.3Å. The QSAR model was validated by predicting activity of test set. A four component PLS factor model with good statistic was obtained for the dataset shown in Table 35. The maximum number of PLS factors in each model can be of 1/5 of the total

number of training set. The atoms visualize 3D characteristics of the ligands (atoms or pharmacophores) as that contributes positively or negatively to activity shown in figure 37. The QSAR model displays 3D characteristics as cubes that represent the model and colour according to the sign of their coefficient values. Positive coefficients indicate an increase in activity, negative coefficients a decrease. The visualization of the coefficients is useful to identify characteristics of ligand structures that tend to increase or to decrease the activity. This might give a clue to what functional groups are desirable or undesirable at certain positions in a molecule.

Table: Statistical Parameter

Factors	SD	R^2	R^2 Scramble	F	P	RMSE	Q^2	Pearson-r
1	0.36	0.61	0.59	26.7	7.72E-05	0.44	0.27	0.65
2	0.26	0.80	0.63	32.9	2.16E-06	0.46	0.32	0.51
3	0.17	0.91	0.64	54.8	2.59E-08	0.43	0.43	0.67
4	**0.11**	**0.97**	**0.77**	**113.4**	**1.68E-10**	**0.41**	**0.57**	**0.82**

Table: Contribution of factors in QSAR

Factors	H-bond donor	Hydrophobic/ non-polar	Electron-withdrawing
1	0.098	0.621	0.281
2	0.107	0.593	0.3
3	0.111	0.589	0.299
4	**0.114**	**0.591**	**0.295**

Validation of QSAR

Validation of a QSAR is the process by which the predictive ability of a QSAR and the mechanistic basis are assessed for practical purpose. There are two techniques to determine reliability of the generated models, internal and external validation.

Internal Validation

Internal validation uses the dataset from which the model is derived and it is required to check internal consistency and stability. To determine quality of the model internal Cross- Validation (CV) techniques is extensively employed. Cross-Validation methods employed as internal validation method are Leave-one-out, Leave-Some-Out or Leave- Many-Out. The quality of the model is analysed by the value of correlation coefficient of the cross-validation procedure, that is, r^2cv. The commonly accepted value for a satisfactory QSAR model is $r^2cv > 0.5$. The most common approach of validation is to examine the residuals which are calculated from difference between observed and predicted biological activity shown in Table 37 and Figure 35.

Table: Residual of Training set molecules

Sr. No.	Experimental activity	Predicted activity	Residual
1 (1A)	8.344	8.30193	-0.0421627
2 (1C)	6.847	6.85076	0.00390806
3 (1D)	7.112	7.06465	-0.0470767
4 (1E)	7.405	7.39345	-0.0111709
5 (1F)	6.789	7.05381	0.265147
6 (1G)	8.246	8.06722	-0.179118
7 (1H)	8.246	8.20955	-0.0367916
8 (1J)	6.852	6.75852	-0.0937424
9 (1L)	7.193	7.28033	0.0869065
10 (1N)	8.324	8.42586	0.101856
11 (1O)	7.304	7.33535	0.0314544

12 (1Q)	7.732	7.65698	-0.0752557
13 (1S)	8.038	8.01295	-0.024634
14 (1T)	7.671	7.61086	-0.0606068
15 (1V)	7.72	7.81408	0.0943839
16 (1W)	7.76	7.82089	0.0607167
17 (1X)	6.575	6.4638	-0.111126
18 (1Y)	7.141	7.1787	0.0378721
19 (1Z)	7.153	7.15273	-0.000560631

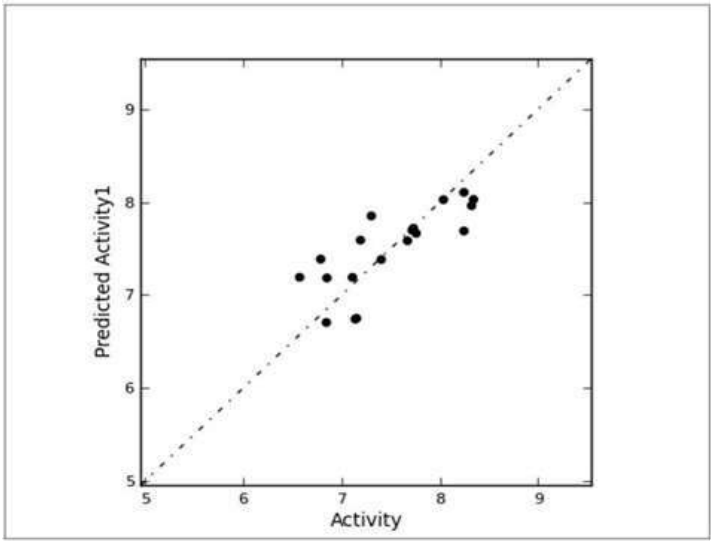

Figure 2 Graph of observed activity versus predicted activity for training set

External Validation

The ultimate validation of the model is examined by means of external validation. The quality of QSAR model is mostly determined by its ability to perform predictions of objects not included in the training sets. The real validation of QSAR model was carried out by examining residuals using test set compounds. The actual activity, predicted activity and residuals for test set compounds are shown in Table 38 and Figure 36.

Table: Residual of Test set molecules

Sr. No.	Experimental activity	Predicted activity	Residual
1 (1B)	8.349	7.96106	-0.388438
2 (1I)	6.864	7.66035	0.796517
3 (1K)	7.75	7.45501	-0.295296
4 (1M)	7.434	7.117	-0.31679
5 (1P)	8.337	7.93468	-0.401902
6 (1R)	7.186	7.44567	0.260093
7 (1U)	7.391	7.4231	0.0323789

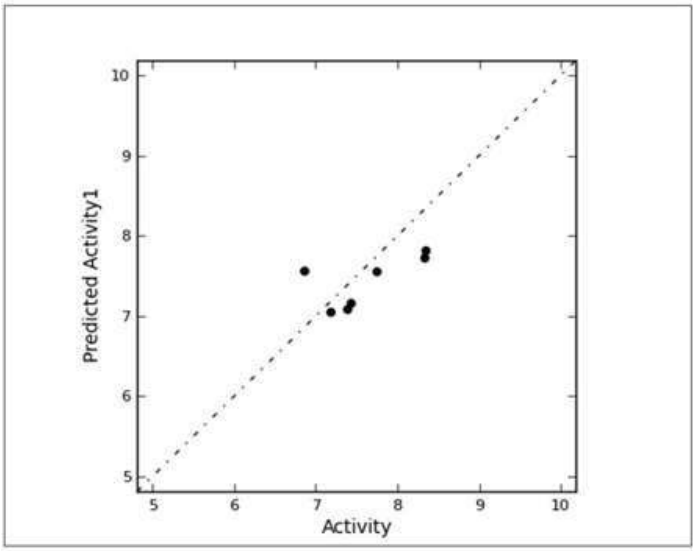

Figure: 3 Graph of observed activity versus predicted activity for test set

Contributing factors in QSAR model

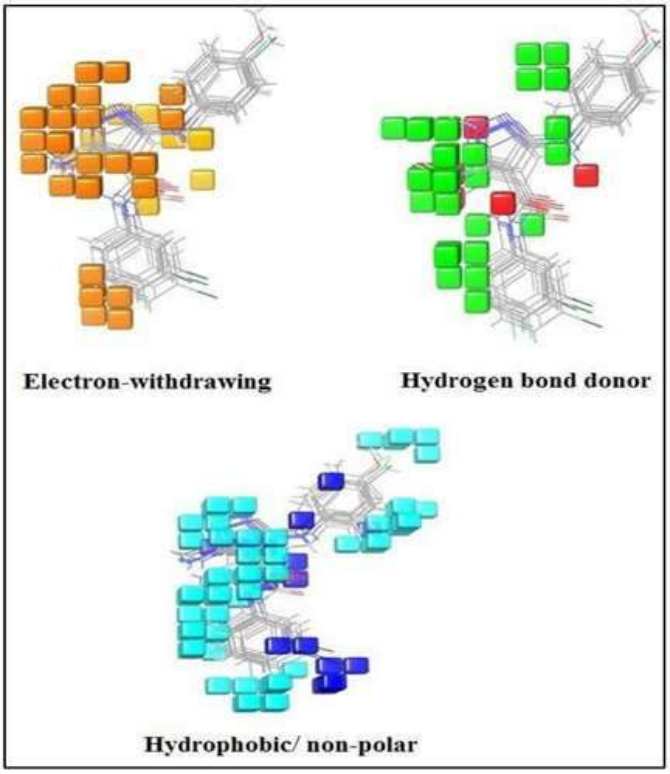

Figure: 4 Description of different factor of QSAR study (A) electrostatic

contribution - Orange cube shows positive contribution while light yellow represent negative contribution

(B) H-bond donor contribution - green cubes represent positive contribution and red represents negative contribution. **(C) Hydrophobic Contribution** - cyan cubes represent positive contribution and dark blue represents negative contribution.

DISCUSSION

A 3D-QSAR analysis was performed on the series of synthesized derivatives to understand the effect of

spatial arrangement of structural features such as H-bond donor, H-bond acceptor, Hydrophobic and electrostatic. The large value of F (113.4) indicates a statistically significant regression model, which is also supported by the small value of the variance ratio (P), an indication of a high degree of confidence. Further, small values of standard deviation (0.11) of the regression and RMSE value of 0.41 makes an obvious implication that the data used for model generation are best for the QSAR analysis. Validity of the model can be expressed by cross-validated correlation coefficient (q^2 = 0.57) that was obtained by leave one out or leave one/some out method. q^2 > 0.5 confirms the model validity. Correlation coefficient of 0.97 suggests good correlation between biological property and structural features. QSAR study indicates that hydrophobic features contribute 59%, electron withdrawing 29% and H-bond donor with 11% (Table 36). Also, lower residual values between experimental and predicted activity suggest reliability and good predictive power of the generated QSAR model (Table 33 and Table 34). Overall QSAR study suggests that hydrophobic property contributes significantly in biological activity. Generated model can be further used for lead modification and optimization to get novel potent molecules. Generated QSAR model was further used for lead modification. Four new molecules were designed and predicted as more potent than the compounds of earlier series (Table 39). These predicted molecules were further subjected to docking studies as discussed in section 4.4. docking scores are shown in Table

Table: Predicted Compounds Fit value and Docking Score

Compound code	Fit value	Docking Score
2I	8.43	-10.113
2H	8.01	-9.57
2G	7.89	-9.01
2F	8.01	-11.13

As predicted compounds are found to have more potency and good docking score. It was planned to synthesize these compounds.

QSAR study on series of 7-hydroxy-5-methyl-*N*-substituted phenyl-2- (substituted phenylamino) pyrazolo[1,5-*a*] pyrimidine-3-carboxamide (LMPM derivatives)

Ligand Preparation and selection of training set

Table: Biological activity of training set molecule

Com. No.	R	R'	MIC	pMIC
1 (1A)	4-OCH3	4-OCH3	12.5	7.525
2 (1B)	4-OCH3	4-Cl	12.5	7.531
3 (1C)	4-OCH3	2,3-di-CH3	50	6.918
4 (1D)	4-OCH3	-H	50	6.891
5 (1G)	4-CH3	4-Cl	3.125	8.116
6 (1H)	-NH2	3,4-di-Cl	6.25	7.749
7 (1I)	-OC2H5	2,4-di-CH3	50	6.936
8 (1K)	2,4-di-CH3	4-OCH3	50	6.291
9 (1L)	2,3-di-CH3	3,4-di-Cl	50	6.959
10 (1M)	4-F	2,4-di-CH3	50	6.909
11 (1N)	2-OCH3	3-CH3	3.125	8.112
12 (1O)	-NH2	4-Cl	50	6.803
13 (1R)	2,3-di-Cl	Piperidine	50	6.954
14 (1S)	2-OCH3	N-Me piperazine	25	7.211
15 (1T)	-H	-H	50	6.857
16 (1U)	-H	4-CH3	100	6.572
17 (1X)	3-Cl 4-F	4-OCH3	50	6.941

18 (1Y)	3-Cl	4-F	50	6.196
19 (1Z)	3-Cl	2,3-di-CH3	50	6.926

Table: Biological activity of test set molecules

Com. No.	R	R'	MIC	pMIC
1 (1E)	4-OCH3	Morpholine	25	7.186
2 (1F)	4-CH3	-H	50	6.873
3 (1J)	4-Cl	2,4-di-CH3	50	6.925
4 (1P)	4-F	3,4-di-F	3.125	8.122
5 (1Q)	-OC2H5	3-CH3	50	6.907
6 (1V)	-H	4-Cl	50	6.896
7 (1W)	3-Cl 4-F	4-CH3	12.5	7.532

QSAR Modelling

Table: Statastical Parameter

Factors	SD	R^2	R^2 Scramble	F	P	RMSE	Q^2	Pearson-r
1	0.33	0.53	0.49	21.5	0.000178	0.22	0.22	0.77
2	0.21	0.82	0.80	42.4	1.55E-07	0.24	0.32	0.32
3	0.12	0.93	0.93	85.5	1.85E-10	0.33	0.37	0.64
4	**0.05**	**0.96**	**0.97**	**160.7**	**2.23E-16**	**0.46**	**0.55**	**0.89**

Table: Contribution of factors in QSAR

Factors	H-bond donor	Hydrophobic non-polar	Electron-withdrawing
1	0.065	0.69	0.242
2	0.072	0.684	0.242
3	0.073	0.686	0.239
4	**0.071**	**0.694**	**0.235**

Validation of QSAR

Internal Validation

Table: Residual of Training set molecules

Sr. No.	Experimental activity	Predicted activity	Residual
1 (1A)	7.525	7.53072	0.00532186
2 (1B)	7.531	7.54017	0.00960324
3 (1C)	6.918	6.94209	0.0238734
4 (1D)	6.891	6.87103	-0.0203994
5 (1G)	8.116	8.04487	-0.0706686
6 (1H)	7.749	7.77659	0.0271131
7 (1I)	6.936	6.94251	0.00679659
8 (1K)	6.921	6.96055	0.0395464
9 (1L)	6.959	6.90284	-0.056161
10 (1M)	6.909	6.88086	-0.0280708
11 (1N)	8.112	8.16207	0.0504749
12 (1O)	6.803	6.84302	0.0399218
13 (1R)	6.954	7.01873	0.0651392
14 (1S)	7.211	7.12739	-0.0834834
15 (1T)	6.857	6.85345	-0.00315634

16 (1U)	6.572	6.5514	-0.0207836
17 (1X)	6.946	6.98853	0.0422421
18 (1Y)	6.916	6.99042	0.0746757
19 (1Z)	6.926	6.83774	-0.0884695

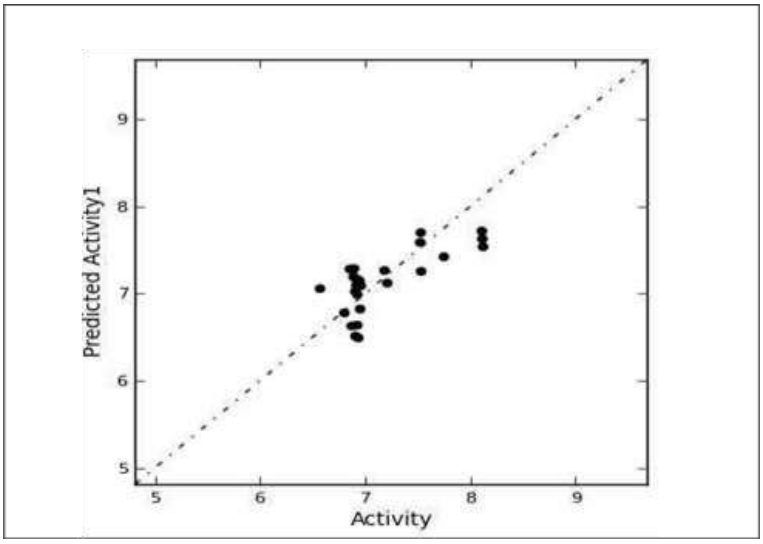

Figure 5 Graph of observed activity versus predicted activity for training set

External Validation

Table 46 Residual of Test set molecules

Sr. No.	Experimental activity	Predicted activity	Residual
1 (1E)	7.186	7.19732	0.0116139
2 (1F)	6.873	6.97293	0.100011
3 (1J)	6.925	7.00673	0.0812863
4 (1P)	8.122	8.09651	-0.0256548
5 (1Q)	6.907	7.00374	0.0967359
6 (1V)	6.896	6.9085	0.0121391
7 (1W)	7.532	7.19596	-0.336376

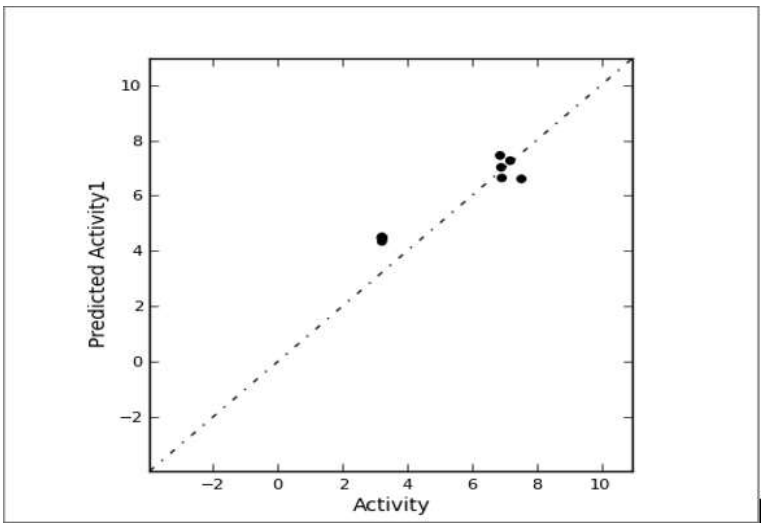

Figure 6 Graph of observed activity versus predicted activity for test set

Contributing factors in QSAR model

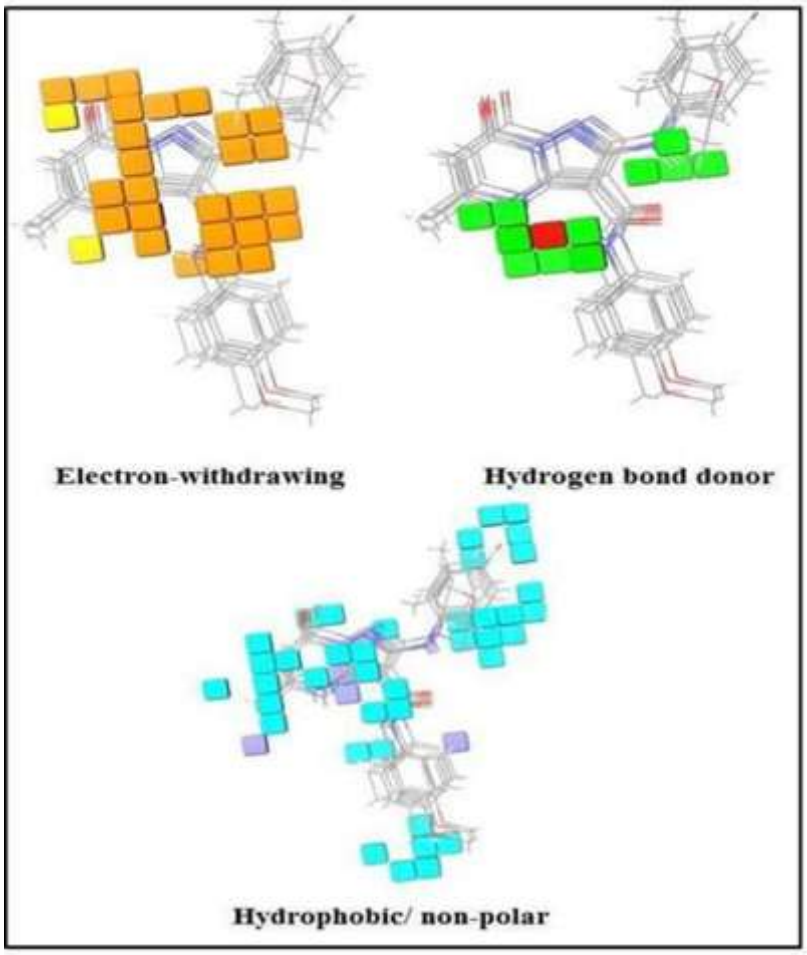

Figure 7 Description of different factor of QSAR study (A) electrostatic contribution -

Orange cube shows positive contribution while light yellow represent negative contribution

(B) H-bond donor contribution - green cubes represent positive contribution and red represents negative contribution. **(C) Hydrophobic Contribution -** cyan cubes represent positive contribution and dark blue represents negative contribution.

DISCUSSION

A 3D-QSAR analysis was performed on the series of derivatives to understand the effect of spatial arrangement of structural features such as H-bond donor, H-bond acceptor, Hydrophobic and electrostatic. The large value of F (160.7) indicates a statistically significant regression model, which is also supported by the small value of the variance ratio (P), an indication of a high degree of confidence. Further, small values of standard deviation (0.05) of the regression and RMSE value of 0.46 makes an obvious implication that the data used for model generation are best for the QSAR analysis. Validity of the model can be expressed by cross-validated correlation coefficient (q^2 = 0.55) that was obtained by leave one out or leave one/some out method. q^2>0.5 confirms the model validity. Correlation coefficient of 0.96 suggests good correlation between biological property and structural features. QSAR study indicates that hydrophobic features contribute 69%, electron withdrawing contributes 23% and H-bond donor contributed 7% (Table 44). Lower residual values between experimental and predicted activity suggest reliability and good predictive power of the generated QSAR model shown in table 41 and table 42. Overall QSAR study suggest that hydrophobic contributes significantly. Generated model can be further used for lead modification and optimization to get novel potent molecules.

Table: Prediction of anti-tuberculosis activity of designed compounds based on model

Predicted compounds	R	R'	Predicted activity
3E	-NH	3-Cl 4-F	9.12809
3C	-NH	4-OCH3	9.08435
3D	4-F	4-F	9.02066
3B	2,4- OCH3	2-OCH3	8.50107
3A	3-Cl 4-F	3-Cl	8.30421

Generated QSAR model was further used for lead modification. Four new molecules were designed and predicted as more potent than the earlier series (Table 47). These predicted molecules were further subjected to docking studies as discussed in section

4.4. docking scores are shown in Table 48.

Table: Predicted Compounds Fit value and Docking Score

Compound code	Fit value	Docking Score
3E	8.327	-8.197
3C	7.134	-8.845
3B	8.025	-9.663
3D	9.28	-10.01
3A	7.59	-8.34

As predicted compounds are found to have more potency and good docking score, it was planned to synthesize these compounds.

CONCLUSION AND SUMMARY

The QSAR study reveals that lipophilicity contributes major role to explain the activity. Electron withdrawing group contribute moderately while hydrogen bond donor found to contribute least. These important parameters can be taken into consideration while designing new inhibitors belonging to the above class of compounds. Generated QSAR model is statistically significant and has excellent predictive power as evidenced from the results of internal and external cross-validation. Results may provide a preliminary valuable guidance for improving the potency of the analogues and continuing search for potent anti- mycobacterial prior to synthesis. Tuberculosis (TB) is a highly contagious infection that has troubled humankind from the history. World Health Organization (WHO) estimates, each year, 8 million people worldwide develop active tuberculosis and nearly 2 million die. The resurgence of TB, accompanied by HIV, has been complicated by the emergence of multiple drug resistant (MDR) and extremely drug resistant (XDR) TB. Recent developments in the therapy of TB have been reviewed. In the present study, we have described the design, synthesis and anti-tubercular evaluation of the series of novel pyrazole and pyrazolo[1,5-*a*]pyrimidine derivatives. Ligand based pharmacophore modeling study was carried out to identify critical features required for specific binding to enoyl-acyl carrier protein reductase, an important enzyme for mycobacterium cell wall synthesis. Pharmacophore model was generated using *Hypogen* module in DS 2.1. Generated pharmacophore model was validated by internal and external validation. The model was found to be statistically significant (r^2 = 0.85) and showed satisfactory Fischer's randomization and cost analysis results. The best model was used for design of novel pyrazole and pyrazolo[1,5-*a*]pyrimidine derivatives. A series of 5-amino-*N*-substituted phenyl-3-(substituted phenylamino)-1*H*- pyrazole- 4-carboxamide (PM) and 7-hydroxy-5-methyl-*N*-substituted phenyl- 2-(substituted phenylamino) pyrazolo [1,5-*a*]pyrimidine-3-carboxamide (LMPM) were designed by considering pharmacophore mapping studies. Based on pharmacophore modelling with good fit values some new molecules of PM and LMPM series were predicted. These molecules were further opted

for molecular docking study with (PDB ID: 2H7M) to verify the fitness of ligand to the target. Molecules with satisfactory docking scores and pharmacophoric fit value were selected for the synthesis. All synthesized derivatives were characterized by physical characteristics like TLC, Melting point and spectral characteristics like IR, Mass, ^{1}H-NMR and ^{13}C- NMR. All synthesized compounds were screened for anti-mycobacterial activity to determine their MIC (Minimum Inhibitory Concentration) by Microplate Alamar Blue Assay (MABA) method on H37Rv strain. Among all synthesized compounds, few compounds have exhibited good anti- mycobacterial activity with MIC values in the range of 0.8–100 µg/mL. Thus, the synthesized compounds can be considered as novel potential anti- mycobacterial candidates. The concept of quantitative structure activity relationship (QSAR) has been briefly reviewed in context of basic principles, and methodologies adopted for QSAR studies. A detailed atom based QSAR study was carried out using both the series, for further lead modification using Schrödinger (Maestro v10.1, Schrodinger, LLC, NEW YORK, NY) software. Results of the QSAR study provided a preliminary valuable guidance for improving the biological activity of the analogues and continuing search for potent anti- mycobacterial agents. Further predicted potent molecules based on QSAR were synthesized, characterized and evaluated for their anti-tubercular activity. Pyrazole analogues shows comparatively good potency against the *Mycobacterium tuberculosis* H37RV strain than pyrazolo[1,5-*a*]pyrimidine derivatives.

REFERENCES

1. Ahmed, N., Boyal, D., Charrier, J. D., Davis, C., Davis, R., Durrant, S., Etxebarriaijardi, G., Jimenez, J. M., Kay, D., Knegtel, R., Middleton, D., Odonnell, M., Panesar, M., Pierard, F., Pinder, J. (2014) Compounds useful as inhibitors of ATR kinase, WO2014089379.
2. Almansa, C., De Arriba, A. F., Cavalcanti, F. L., Gómez, L. A., Miralles, A., Merlos, M., Garcia-Rafanell, J., Forn, J. (2001) Synthesis and SAR of a new series of COX-2-selective inhibitors: Pyrazolo[1,5-a] pyrimidines, J. Med. Chem., 44, 350–361.
3. Altare, F., Jouanguy, E., Lamhamedi-Cherradi, S. (1998) A causative relationship between mutant IFNgR1 alleles and impaired cellular response to IFN gamma in a compound heterozygous child, American Journal of Human Genetics, 62, 723–726.
4. Andrew S., Steven L. Teig, P. (1995) Towbin Poling: Promoting conformational variation, 16, 171–187.
5. Andries, K., Verhasselt, P., Guillemont, J. A. (2005) Diarylquinoline drug active on the ATP synthase of Mycobacterium tuberculosis, Science, 307, 223- 227.
6. Andrews, S. W., Condroski, K. R., Demeese, L. A., Fell, J. B., Fischer, J. P., Lehuerou, Y., Josey, J. A., Koch, K., Miknis, G. F., Rodriguez, M. E., Topalov, G. T., Wallace, E. M., Xu, R. (2011) Substituted pyrazolo[1,5-a] pyrimidine compounds as mTOR inhibitors, WO2011029027.
7. Anil, K., Axel, C. (2001) Serine/threonine protein kinases PknF and PknG of Mycobacterium tuberculosis characterization and localization, Microbiology,147, 2307–2314.
8. Antigone, B. (2012) NIH-funded TB drug trial is latest effort to fill treatment pipeline, Science Speaks: Global ID News, December 12.
9. Armstrong, J. A. and Hart, P. D. (1775) Phagosome-lysosome interactions in cultured macrophages infected with virulent tubercle bacilli, Reversal of the usual non-fusion pattern and observation on bactericidal survival, Journal of Experimental Medicine, 142, 1-16.
10. Arif, B. S., Amit, T., Vipul, B. K., Viresh, H. S. (2014) 4,5-Dihydro-1H- Pyrazolo[3,4-d]pyrimidine containing Phenothiazines as Antitubercular Agents, Med. Chem. Res., 12, 314- 319.
11. Asselineau J, Lederer E. (1950) Structure of the Mycolic Acids of Mycobacteria, Med. Chem. Res., 166, 782–783.
12. Bales, P. M., Renke, E. M., May, S. L., Shen, Y., Nelson, D. C. (2013) Purification and characterization of biofilm-associated EPS exopolysaccharides from ESKAPE organisms and other pathogens, PLoS One, 8, 67950.
13. Bale, T. L. (2006) Stress sensitivity and the development of affective disorders, Horm. Behav., 50, 529-533.

14. Banerjee, A., Dabnau, E., Quemard, A., Balasubramanian, V., Um, K. S., Wilson, T., Collins, D., De, G., Hacobs, W. R. (1994) Inh A. A gene encoding a target for isonisazid and ethionamide in mycobacterium tuberculosis, Science, 263, 227-230.
15. Basoff, I. M., Barry, C. E. (2005) Tuberculosis Metabolism and respiration in the absence of growth, Nat. Rev. Microbiol., 3, 70-80.
16. Bearss, D. J., Xiao-Hui, L., Hariprasad, V., Yong, X. (2014) Imidazo[1,2- b]pyridazine and pyrazolo[1,5-a]pyrimidine derivatives and their use as protein kinase inhibitors. US8710057.
17. Berger, D. M., Torres, N., Dutia, M., Powell, D., Ciszewski, G., Gopalsamy, A., Levin, J. I., Kim, H., Xu, W., Wilhelm, J., Hu, Y., Collins, K., Feldberg, L., Kim, S., Frommer, E., Wojcichowicz, D., Mallon, R. (2009) Non-hinge-binding pyrazolo[1,5-a]pyrimidines as potent B-Raf kinase inhibitors, Bioorg. Med. Chem. Let., 19, 6519-6523.
18. Bernann P. J. (2003) Structure, function and biogenesis of the cell wall of Mycobacterium tuberculosis, Tuberculosis, 83, 91-97.
19. Besra, G. S., Brennan, P. J. (1997) The mycobacterial cell envelope: a target for novel drugs against tuberculosis, Journal of Pharmacy and Pharmacology, 49, 25-30.
20. Bhadti, V. S. Ph.D. Thesis (1985) Studies on the synthesis of pyrimidines from ketene thioacetals and condensed pyrimidines from o-aminonitriles by the reaction with nitriles under acidic condition, Gujarat University.
21. Bharatham, N., Lee, K. W. (2007) Pharmacophore identification and virtual screening for methionyl-tRNA synthetase inhibitors, Journal of Molecular Graphics & Modeling, 25, 813– 823.
22. Bhatt, A., Kremer, L., Dai, A. Z., Sacchettini, J. C., Jacobs, W. R Jr. (2005) Conditional depletion of KasA, a key enzyme of mycolic acid biosynthesis, leads to mycobacterial cell lysis, Journal of Bacteriology, 187, 7596–7606.
23. Bishai, W. R., Chaisson, R. E. (1997) Shoet-course chemoprphylaxis for tuberculosis, Clin. Chest Med., 181, 115-122.
24. Bocchino, M., Sanduzzi, A., Bariffi, F. (2000) Mycobacterium tuberculosis and HIV co-infection in the lung: synergic immune dysregulation leading to disease progression, Monaldi Archives for Chest Disease, 55, 381–388.
25. Bondock, S., Rabie, R., Etman, H. A., Fadda, A. A. (2008) Synthesis and antimicrobial activity of some new heterocycles incorporating antipyrine moiety, Eur. J. Med. Chem., 43, 2122–2129.
26. Boyer, S. J. (2002) Small molecule inhibitors of KDR (VEGFR-2) kinase: an overview of structure activity relationships, Curr. Top. Med. Chem., 2, 973– 1000.
27. Braestrup, C., Squires, R.F. (1977) Specific benzodiazepine receptors in rat brain characterized by high-affinity [3H] diazepam binding, Proc. Natl. Acad. Sci., 74, 3805–3809.
28. Brennan, P.J., Draper, P. (1994) In tuberculosis pathogenesis, protection and control, Bloom BR Ed., American society for Microbiology, Washington DC, 271-284.
29. Brooks, B. R., Bruccoleri, R. E., Olafson, B. D., States, D. J., Swaminathan, S., Karplus, M. (1983) CHARMM: A program for macromolecular energy, minimization, and dynamics calculations, Journal of Computational Chemistry, 4, 187–217.
30. Cancers, N. E., Harris, N. B., Wellehan, J. F., Feng, Z., Kapur, V., Barlettaet, R. G. (1997) Overexpression of the D-alanine racemase gene confers resistance to D-cycloserine in Mycobacterium smegmtis, J. Bacterion., 179, 5046-5055.
31. Cardona, P. J., Manzanoj, R. (2004) On the nature of Mycobacterium tuberculosis bacilli,Eur. Respir. J., 24, 1044-1051.
32. Chen, P., Gearhart, J., Protopopova, M., Einck, L., Nacy, C. A. (2006) Synergistic interactions of SQ109, a new ethylene diamine, with front-line antitubercular drugs in vitro, Journal of Antimicrobial Chemotherapy, 58, 332- 337.

Cite: Bargaje Goraksh*, Rajeev Kumar Malviya, Design Synthesis and Development of Some Novel Pyrrole Derivatives as Antitubercular Agents, Int. J. Med. Pharm. Sci., 2026, 2 (9), 1-27. https://doi.org/10.5281/zenodo.22244992